RECURSIVE INTEGRAL METHOD FOR THE NONLINEAR NON-SELFADJOINT TRANSMISSION EIGENVALUE PROBLEM*

Yingxia Xi   and   Xia Ji

LSEC, NCMIS, Institute of Computational Mathematics, Academy of Mathematics and Systems Science, Chinese Academy of Sciences, Beijing 100190, China
Email: yxiaxi@lsec.cc.ac.cn, jixia@lsec.cc.ac.cn

Abstract

The transmission eigenvalue problem is an eigenvalue problem that arises in the scattering of time-harmonic waves by an inhomogeneous medium of compact support. Based on a fourth order formulation, the transmission eigenvalue problem is discretized by the Morley element. For the resulting quadratic eigenvalue problem, a recursive integral method is used to compute real and complex eigenvalues in prescribed regions in the complex plane. Numerical examples are presented to demonstrate the effectiveness of the proposed method.

Mathematics subject classification: 34L16, 65L60.
Key words: Transmission eigenvalue problem, Nonlinear eigenvalue problem, Contour integrals.

1. Introduction

The transmission eigenvalue (TE) problem has important applications in inverse scattering theory and has attracted attention of many researchers recently [3, 4, 7–9, 25]. Although stated in a simple form, the TE problem is nonstandard and not covered by classical theories.

In this paper, we consider the numerical treatment of the TE problem. The first effort was given in [8], where three finite element methods (FEM) were proposed. Two iteration methods were proposed with rigorous convergence analysis in [23]. A mixed method was developed in [13]. An efficient spectral element based numerical method for the 2D TE problem of radially stratified media was given in [1]. Recently, a mixed FEM with convergence proof was proposed to solve the TE problem in [5], and another FEM based method, which transforms the TE problem into a quadratic eigenvalue problem (QEP), was given in [19]. The related source problem [10, 26] and other multilevel [12] and multigrid [14] type methods have also been discussed.

Some non-traditional methods, such as the linear sampling method [24] and the inside-out duality method [18], have been applied to estimate TEs using scattering data. However, these methods need to solve a tremendous number of direct problems which make them computationally prohibitive.

Recently, contour integral based methods have been successfully applied to solve eigenvalue problems. In [21, 22], a contour integral based method was proposed to compute eigenvalues of a generalized eigenvalue problem, which lie in a specific region in the complex plane. And in [2], a contour integral based method was used to solve a nonlinear eigenvalue problem (NEP)

---

by formulating the NEP as a linear eigenvalue problem (LEP). In [17], a contour integral based method was used to compute TEs in a special case when the index of refraction is a constant. In [11], a novel recursive integral method (RIM) was proposed to solve LEPs. Based on the eigenprojections of compact operators, regions are searched recursively to test whether there exist eigenvalues lying inside a specific contour in the complex plane. RIM is effective, robust, and essentially parallelizable. According to [11], even for the case when the matrix is non-Hermitian and degenerate, and the information of the spectrum structure is unknown, RIM still works successfully.

This paper focuses on the extension of RIM to solve NEPs and numerically shows its robustness. We derive the formulation of RIM for a QEP. Both real and complex eigenvalues are computed effectively. We discretize the TE problem by the nonconforming Morley element. For the derived QEP, we employ RIM to find both real and complex eigenvalues within a specific contour in the complex plane. The TE problem is indeed a fourth order problem [4]. Writing it in a mixed form as in [11] would require higher regularity of eigenfunctions which in turn leads to a restriction of the domain, see, e.g., Chp. 4 of [25]. It is known that a similar mixed finite element approach for the biharmonic equation leads to spurious eigenvalues, which could happen when the domain is non-convex. Hence it is preferable to discretize the weak formulation directly and the Morley element is a suitable non-conforming element for triangular meshes. We only provide a theoretical proof for the Morley element when the refractive index $n(x)$ is a constant [15], while the proof for more general case when $n(x)$ is non-constant is still open.

This paper is organized as follows. In Section 2, we introduce the TE problem, the reduced fourth order formulation and the corresponding nonconforming FEM discretization. In Section 3, RIM for the QEP is given. In Section 4, numercial examples are presented to validate the algorithm. Section 5 is the conclusion part.

2. The Transmission Eigenvalue Problem

2.1. Formulation

For the scattering of time-harmonic acoustic waves by a bounded and simply connected inhomogeneous medium $\Omega \subset \mathcal{R}^2$, the transmission eigenvalue problem is to find $k \in \mathcal{C}$ and $\phi, \varphi \in H^2(\Omega)$ such that

$$\begin{cases} \Delta\phi + k^2 n(x)\phi = 0, & \text{in } \Omega, \\ \Delta\varphi + k^2\varphi = 0, & \text{in } \Omega, \\ \phi - \varphi = 0, & \text{on } \partial\Omega, \\ \frac{\partial\phi}{\partial\nu} - \frac{\partial\varphi}{\partial\nu} = 0, & \text{on } \partial\Omega, \end{cases} \tag{2.1}$$

where ν is the unit outward normal to the boundary $\partial\Omega$. The index of refraction $n(x)$ is either $n(x) > \alpha_0$ a.e. in Ω for some constant $\alpha_0 > 1$, or $0 < n(x) < \tilde{\alpha}_0$ a.e. in Ω for some constant $\tilde{\alpha}_0 < 1$. Here we consider the first case. The second one follows similarly. Complex number k for which there exists a nontrivial solution to (2.1) is called a TE [8].

We define

$$V := H_0^2(\Omega) = \left\{ u \in H^2(\Omega) : \ u = 0 \text{ and } \frac{\partial u}{\partial \nu} = 0 \text{ on } \partial\Omega \right\},$$

and denote (u, v) the $L^2(\Omega)$ inner product. Introducing a new variable $u = \phi - \varphi \in V$ and following the same procedure in [13], one finds that u and k satisfy the fourth order problem

$$\left(\Delta + k^2 n(x)\right) \frac{1}{n(x) - 1} (\Delta + k^2) u \quad = \quad 0. \tag{2.2}$$

(2.2) can be formulated in weak form: Find $(k^2 \neq 0, u) \in \mathcal{C} \times V$ such that

$$\left(\frac{1}{n(x)-1}(\Delta u + k^2 u), \Delta v + k^2 n(x)v\right) = 0, \quad \forall v \in V. \tag{2.3}$$

Denoting $\tau = k^2$, we rewrite (2.3) as

$$\left(\frac{1}{n(x)-1}(\Delta u + \tau u), \Delta v + \tau n(x)v\right) = 0, \quad \forall v \in V. \tag{2.4}$$

2.2. The Morley element

The Morley element is the simplest nonconforming element for the fourth order problem [20]. Let $\mathcal{T}_h$ be a shape regular triangular mesh over Ω, which means there exists a constant γ such that

$$\frac{h_K}{\rho_K} \leq \gamma, \quad \forall K \in \mathcal{T}_h, \tag{2.5}$$

where h_K denotes the diameter of the smallest ball containing K, and ρ_K is the diameter of the biggest possible ball contained in K, $h := \max\{h_K : K \in \mathcal{T}_h\}$.

The Morley element is defined as follows

$$V_h = \Big\{v \in L^2(\Omega): \; v|_K \in \mathcal{P}_2(K), \; v \text{ and } \partial_\nu v \text{ are continuous at vertices and}$$

$$\text{the midpoints of edges respectively and vanish on the boundary } \partial\Omega\Big\},$$

where $\mathcal{P}_2(K)$ denotes the space of polynomials whose degree is less than or equal to two.

We assume $0 < \alpha_s \leq \frac{1}{n(x)-1} \leq \alpha_b$. Before discretizing the fourth order problem (2.4) by the Morley element, the following formulations for $u, v \in H_0^2(\Omega)$ are introduced [6]

$$\begin{cases} \left(\frac{1}{n(x)-1}\Delta u, \Delta v\right) = \left(\left(\frac{1}{n(x)-1} - \alpha\right)\Delta u, \Delta v\right) + (\alpha\nabla^2 u, \nabla^2 v), \\ \left(\frac{n(x)}{n(x)-1}\Delta u, v\right) + \left(\frac{1}{n(x)-1}u, \Delta v\right) = \left(\frac{1}{n(x)-1}\Delta u, v\right) + \left(\frac{1}{n(x)-1}u, \Delta v\right) - (\nabla u, \nabla v), \\ \left(\frac{1}{n(x)-1}u, n(x)v\right) = \left(\frac{n(x)}{n(x)-1}u, v\right), \end{cases} \tag{2.6}$$

where $(\nabla^2 u, \nabla^2 v) = \int_\Omega \sum_{s,t=1}^2 \frac{\partial^2 u}{\partial x_s \partial x_t} \frac{\partial^2 v}{\partial x_s \partial x_t} dx$, i.e., the inner product of the Hessian matrices of u and v, α is a constant satisfying $0 < \alpha < \alpha_s$.

Define the bilinear form

$$a(u,v) = \left(\left(\frac{1}{n(x)-1} - \alpha\right)\Delta u, \Delta v\right) + (\alpha\nabla^2 u, \nabla^2 v). \tag{2.7}$$

We have

$$\alpha\|\nabla^2 u\|_{0,\Omega}^2 \leq a(u,u) \leq \alpha_b\|\nabla^2 u\|_{0,\Omega}^2. \tag{2.8}$$

Denote the norm $\|u\|_* = \sqrt{a(u,u)}$. Then it is equivalent to $\|u\|_{2,\Omega}$ since $u \in H_0^2(\Omega)$.

The discrete problem is to find $\tau_h \in \mathcal{C}$ and $u_h \in V_h$ such that

$$a_h(u_h, v_h) + \tau_h b_h(u_h, v_h) + \tau_h^2 c_h(u_h, v_h) = 0, \quad \forall v_h \in V_h, \tag{2.9}$$

where

$$\begin{cases} a_h(u_h, v_h) = \sum_{K \in \mathcal{T}_h}\left(\left(\frac{1}{n-1} - \alpha\right)\Delta u_h, \Delta v_h\right)_K + (\alpha\nabla^2 u_h, \nabla^2 v_h)_K, \\ b_h(u_h, v_h) = \sum_{K \in \mathcal{T}_h}\left(\frac{1}{n-1}\Delta u_h, v_h\right)_K + \left(\frac{1}{n-1}u_h, \Delta v_h\right)_K - (\nabla u_h, \nabla v_h)_K, \\ c_h(u_h, v_h) = \left(\frac{n}{n-1}u_h, v_h\right). \end{cases} \tag{2.10}$$

It is easy to show that

$$\alpha \sum_{K \in \mathcal{T}_h} \|\nabla^2 u_h\|_{0,K} \le a_h(u_h, u_h) \le \alpha_b \sum_{K \in \mathcal{T}_h} \|\nabla^2 u_h\|_{0,K}, \tag{2.11}$$

and that $\|u_h\|_{*,h} = \sqrt{a(u_h, u_h)}$ is a norm on V_h. If $u \in H_0^2(\Omega)$, $\|u\|_{*,h} = \|u\|_*$.

Then we have the following QEP:

$$(A + \tau B + \tau^2 C)x = 0, \tag{2.12}$$

where A, B and C are the matrices associated with $a_h(\cdot, \cdot)$, $b_h(\cdot, \cdot)$ and $c_h(\cdot, \cdot)$ respectively.

3. A Recursive Contour Integral Method

Equation (2.12) is nonlinear and has complex eigenvalues. In addition, the spectrum is very complicated. There is no estimation on the number and multiplicity of eigenvalues in a region in the complex plane. In this section, we introduce the idea of RIM which doesnot require any priori information of the spectrum and extend it to solve the QEP (2.12).

Let $T(\tau) := A + \tau B + \tau^2 C$, (2.12) can be written as

$$T(\tau)x = 0, \ x \ne 0. \tag{3.1}$$

Then T is holomorphic in some open domain [2]. We denote $\sigma(T)$ the set of all eigenvalues and $\rho(T) = \mathcal{C} \backslash \sigma(T)$ the resolvent set.

We first recall some classical results of linear operator theory (see, e.g., [16]). We assume that $T : X \to X$ is a linear operator on the complex Hilbert space X. Γ is a simply closed curve in the complex plane which encloses m eigenvalues, counting multiplicity, of $T : \lambda_j, j = 1, \cdots, m$. The operator

$$P(T) = \frac{1}{2\pi i} \int_\Gamma (z - T)^{-1} dz, \tag{3.2}$$

is a projection on the space generated by generalized eigenfunctions $\mathbf{u}_j, j = 1, \cdots, m$ associated with $\lambda_j, j = 1, \cdots, m$.

Based on this property, Huang et al. [11] proposed RIM to find eigenvalues lying inside a specific contour in the complex plane. The idea of RIM is to use $P(T)f$ to determine whether Γ encloses eigenvalues of T. For a random $f \in X$, if there are eigenvalues inside Γ, $P(T)f \ne 0$. Otherwise, $P(T)f = 0$.

Generally, for the nonlinear operator, the projection operator does not have this good property. But for the NEP (3.1) considered here, T is a holomorphic operator. Based on Theorem 2.4 and Theorem 2.9 in [2], the operator

$$P(T) = \frac{1}{2\pi i} \int_\Gamma T(z)^{-1} dz, \tag{3.3}$$

is also a projection onto the space of generalized eigenfunctions associated with eigenvalues inside Γ. In fact, as in [2], for the simple eigenvalue case, let $\mathbb{C} \subset X$ be a compact subset that contains $\lambda_j, j = 1, \cdots, m$. Then there is a neighborhood U of $\mathbb{C}$ in X

$$T(z)^{-1} = \sum_{j=1}^{m} \frac{1}{z - \lambda_j} v_j w_j^H + R(z), \ z \in U \backslash \{\lambda_1, \cdots, \lambda_m\}, \tag{3.4}$$

where v_j and w_j are related eigenfunctions, and $R(z)$ is a holomorphic function. So we have

$$P(T) = \frac{1}{2\pi i} \int_\Gamma T(z)^{-1} dz = \sum_{j=1}^{num(\Gamma)} v_j w_j^H, \tag{3.5}$$

where $num(\Gamma)$ is the number of eigenvalues inside Γ. These are results for simple eigenvalues. Similar results can be obtained for more complicated cases [2]. This implies that we can also choose a random f and compute $P(T)f$. $P(T)f = 0$ means no eigenvalues inside Γ. Otherwise there are eigenvalues.

RIM tries to find all the eigenvalues to a certain precision inside Γ recursively. Let S be the interior of Γ. If S contains eigenvalues, we partition S into subdomains and repeat this procedure for each subdomain until each eigenvalue is isolated.

Next, we will present some details about the numerical implementation.

3.1. Integral approximation

To solve equation (3.1), we need to compute the contour integral (3.3), where Γ is a simply closed curve in the complex plane. Let $\{z_k, p_k\}$, $k = 1, \cdots, N$, be a suitable quadrature rule for Γ, such as the Guass-Legendre quadrature. The projection operator (3.3) is approximated using

$$P(T) \approx \frac{1}{2\pi i} \sum_{k=1}^N p_k T(z_k)^{-1}, \tag{3.6}$$

where z_k and p_k, $k = 1, \cdots, N$, are nodes and weights of the quadrature, respectively.

The projection of a random vector f can be approximated by

$$P(T)f \approx \frac{1}{2\pi i} \sum_{k=1}^N p_k T(z_k)^{-1} f. \tag{3.7}$$

We denote

$$\begin{cases} \omega_k = \frac{1}{2\pi i} p_k, \\ r_k = T(z_k)^{-1} f, \end{cases} \quad k = 1, \cdots, N. \tag{3.8}$$

Note that (3.7) can be written as

$$P(T)f \approx \sum_{k=1}^N \omega_k r_k. \tag{3.9}$$

In practice, we do not compute $T(z_k)^{-1}$ explicitly. Instead, we get r_k by solving the following linear system

$$T(z_k) r_k = f, \quad k = 1, \cdots, N. \tag{3.10}$$

3.2. Algorithm for NEP

RIM in Huang et al. [11] is adopted for the NEP (3.1). We try to compute all eigenvalues of (3.1) in the interior of Γ, i.e., S, using the spectral projection of a random vector $P(T)f$. If $P(T)f = 0$, then S contains no eigenvalues. Otherwise, S contains one or more eigenvalues. Then we partition the region into subregions. For every subregion, we repeat this procedure recursively until the subregion is small enough to isolate each eigenvalue. The computation process is shown in Algorithm 3.1.

Algorithm 3.1. RIM$(N, \Gamma, f, \varepsilon)$ for NEP (3.1).

  Input:

    The number of quadrature nodes: N (points: z_k and weights: p_k);

    Search region: Γ;

    The random vector: f;

    Tolerance: ε.

  Output:

    The eigenvalue(s) inside Γ.

    Approximate the integral by Guass-Legendre formula;

    Compute $\omega_k = \frac{1}{2\pi i} p_k, \ k = 1, \cdots, N$;

    Solve $r_k: \ \ T(z_k) r_k = f, \ k = 1, \cdots, N$;

    $P(T)f \approx \sum_{k=1}^{N} \omega_k r_k$.

    Determine the existence of eigenvalue(s) in Γ;

    if Γ contains eigenvalue(s), **then**

      compute the domain size $h(\Gamma)$.

      if $h(\Gamma) > \varepsilon$, **then**

        partition Γ into subdomains $\Gamma_j, (j = 1, \cdots, L)$,

        RIM$(N, \Gamma_j, f, \varepsilon)$.

      else

        output eigenvalue(s) and exit.

      end if

    end

We use $||P(T)f||$ to decide if a region contains eigenvalues. If $||P(T)f|| = O(1)$, there exists at least one eigenvalue in Γ. If $P(T)f = o(1)$, there is no eigenvalue. However, if the projection of f onto the range of $P(T)$ is small, $||P(T)f||$ can be relatively small while there is an eigenvalue(s). The solution to avoid missing possible eigenvalues is to project $P(T)f$ once again and set the indicator [11]

$$\sigma = \left|\left| P(T) \left(\frac{P(T)f}{||P(T)f||} \right) \right|\right|. \tag{3.11}$$

Here $\sigma = 1/10$ is used as the threshold value.

If there exist eigenvalues lying outside Γ but very close to it, $||P(T)f||$ can be relatively large. In fact, this must happen when RIM zooms into the neighborhood of an eigenvalue. Fortunately, RIM has an interesting self-correction property that fixes such errors on the subsequent iterations [11].

Here are some details in the numerical implementation: the search region is a rectangle; Matlab '\' is used to solve the linear system; one point quadrature is used for each edge of Γ; one random vector f is used; and f is projected twice to compute the indicator (3.11).

4. Numerical Examples

In this section, we present some numerical examples. Using the Morley element, we obtain a QEP as described in section 2. Then we use RIM (Algorithm 3.1) to compute eigenvalues. Mesh size $h \approx 0.05$ and tolerance $\varepsilon = 1e - 3$ are used in all the exmaples.

4.1. The model of a disk

In this subsection, we consider the case when the region Ω is a disk. In **Example 4.1**, the index of refraction is a constant such that the exact TEs are available via special functions [8].

Example 4.1. The region Ω is a disk with radius $R = \frac{1}{2}$ and $n(x) = 16$.

The first search region is $S_1 = [3,7] \times [-1,1]$ which contains only real eigenvalues [8]. The computational results are

$$\lambda_1 = 3.958984, \ \lambda_2 = 6.819922, \ \lambda_3 = 6.820703,$$

which are good approximations to the exact TEs [8]

$$\lambda_1 = 3.952125, \ \lambda_2 = 6.827403, \ \lambda_3 = 6.827403.$$

The second region is $S_2 = [22,25] \times [4,7]$ containing a complex eigenvalue $23.684298 + 5.666293i$ [8]. The numerical result by RIM is

$$\lambda = 23.973511 + 6.514771i.$$

The exact eigenvalue of the QEP (2.12) is

$$\lambda = 23.973791 + 6.514444i,$$

which is obtained by transforming (2.12) to a generalized matrix eigenvalue problem and solving it directly.

Explored regions by RIM are plotted in Fig 4.1. The algorithm refines near eigenvalues until the precision is met. Search region S_1 is shown on the left and S_2 on the right. For S_1, the picture seems to have only two eigenvalues because λ_2 and λ_3 are very close.
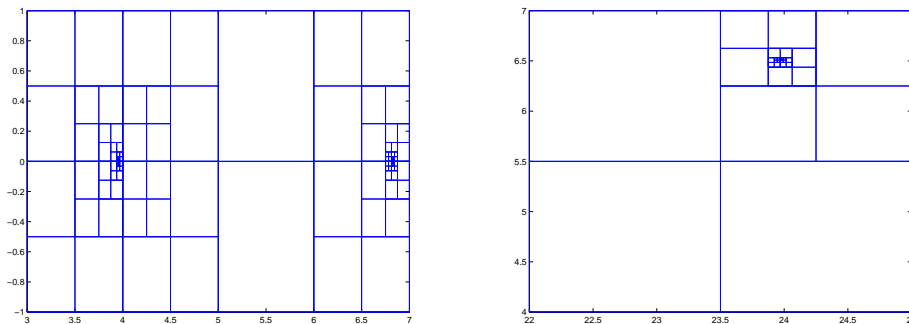
Fig. 4.1. Explored regions by RIM when the model is a disk with radius $R = \frac{1}{2}$ and $n(x) = 16$. Left: S_1, right: S_2.

Example 4.2. The radius of disk R is still $\frac{1}{2}$ and the index of refraction $n(x) = 8 + 4|x|$.

Numerical results are shown in Table 4.1. "Nums" are computed eigenvalues using our proposed method. "QEPs" are the exact eigenvalues of QEP (2.12). The TEs in S_3 are consistent with the results in [13].

Search regions are shown in Fig 4.2. The left picture is for S_3 and the right for S_4.

Table 4.1: Numerical results for the disk with $n(x) = 8 + 4|x|$.

$S_3 = [7, 13] \times [-1, 1]$	Nums:	7.263184, 12.206543, 12.206543
	QEPs:	7.263081, 12.206233, 12.206827
$S_4 = [22, 25] \times [6, 9]$	Nums:	$22.437622 + 8.025513i$
	QEPs:	$22.437461 + 8.025297i$
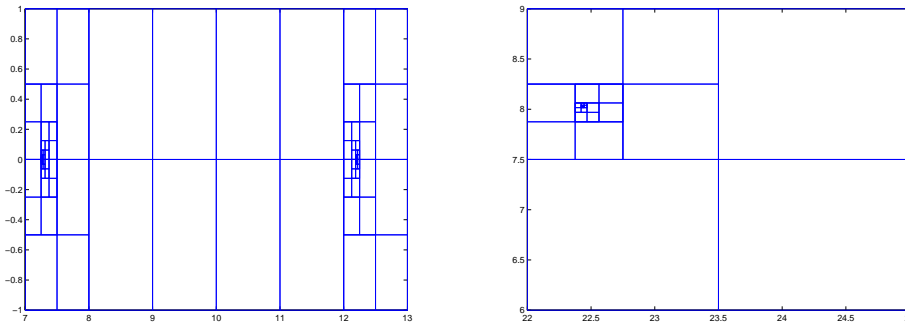
Fig. 4.2. Explored regions when the inhomogeneous medium is a disk with radius $R = \frac{1}{2}$ and $n(x) = 8 + 4|x|$. Left: S_3; right: S_4.

4.2. The model of the unit square

Example 4.3. We consider the unit square and the index of refraction $n(x) = 16$.

Numerical results are given in Table 4.2. The TEs in S_5 are consistent with the results in $[13, 14]$.

Table 4.2: Results for the unit square with $n(x) = 16$.

$S_5 = [3, 7] \times [-1, 1]$	Nums:	3.521973, 5.939941, 5.939941
	QEPs:	3.521718, 5.939796, 5.940268
$S_6 = [20, 25] \times [4, 9]$	Nums:	$20.379944 + 5.739807i$
	QEPs:	$20.380061 + 5.740217i$

Example 4.4. The unit square with the non-constant refractive index.

For different regions, numerical results are shown in Table 4.3 and Table 4.4. For the case of $n(x) = 8 + x_1 - x_2$ and region S_7, TEs are consistent with the results in $[13, 14]$.

4.3. The model of a L-shaped domain

We consider a L-shaped domain $\Omega = (-1, 1) \times (-1, 1) \backslash [0, 1) \times (-1, 0]$ which has a reentrant corner.

Example 4.5. We consider the L-shaped domain with $n(x) = 16$.

For different regions, numerical results are shown in Table 4.5.

We plot search regions in Fig 4.3. The left picture is for S_{13} and the right for S_{14}.

Table 4.3: Numerical results of the unit square for different indices of refraction, where $S_7 = [7, 13] \times [-1, 1]$, $S_8 = [22, 30] \times [-1, 1]$, $S_9 = [7, 13] \times [-1, 1]$.

$n_1(x) = 8 + x_1 - x_2$	S_7	Nums:	7.955566, 12.474121, 12.477051
		QEPs:	7.955378, 12.473438, 12.476424
$n_2(x) = x_1^2 + x_2^2 + 4$	S_8	Nums:	23.844238, 24.020020, 29.641114
		QEPs:	23.844089, 24.020532, 29.640673
$n_3(x) = x_1 x_2 + 8$	S_9	Nums:	7.636230, 12.022949, 12.090332
		QEPs:	7.636272, 12.022476, 12.089943

Table 4.4: Numerical results of the unit square for different indices of refraction, where $S_{10} = [18, 20] \times [7, 9]$, $S_{11} = [16, 18] \times [6, 8]$, $S_{12} = [18, 20] \times [7, 9]$.

$n_1(x) = 8 + x_1 - x_2$	S_{10}	Nums:	$19.414551 + 8.143066i$
		QEPs:	$19.414628 + 8.142981i$
$n_2(x) = x_1^2 + x_2^2 + 4$	S_{11}	Nums:	$17.349121 + 7.509277i$
		QEPs:	$17.349516 + 7.509845i$
$n_3(x) = x_1 x_2 + 8$	S_{12}	Nums:	$19.256348 + 8.010254i$
		QEPs:	$19.256458 + 8.010978i$

Table 4.5: Experimental results of the L-shaped domain.

$S_{13} = [3, 5] \times [-1, 1]$	Nums:	3.171387, 3.562012, 4.465332, 4.514160
	QEPs:	3.171263, 3.561767, 4.465585, 4.513660
$S_{14} = [8, 10] \times [2, 4]$	Nums:	$9.370605 + 3.440918i$
	QEPs:	$9.370494 + 3.440953i$
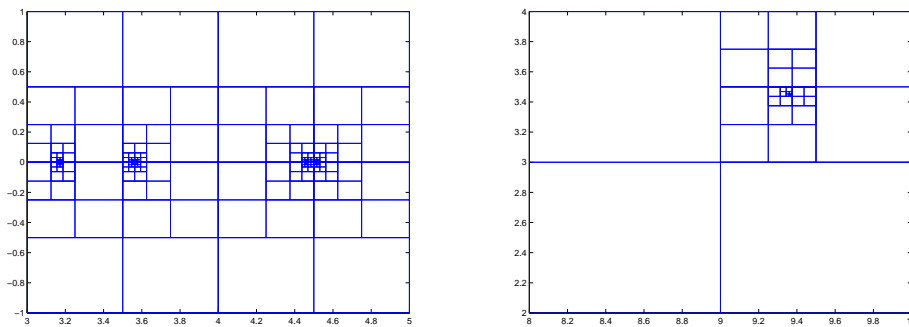
Fig. 4.3. Explored regions for the L-shaped domain with $n(x) = 16$. Left: S_{13}, right: S_{14}.

5. Conclusion

In this paper, we extend the recursive integral method to nonlinear eigenvalue problems and numerically show its robustness. By using a fourth order formulation, the transmission eigenvalue problem is discretized by the Morley element. The recursive integral method was applied to solve the resulting quadratic eigenvalue problem. Using the proposed method, both real and complex eigenvalues can be obtained in prescribed regions in the complex plane effectively.

References

[1] J. An and J. Shen, A spectral-element method for transmission eigenvalue problems, *J. Sci. Comput.*, **57** (2013), 670-688.

[2] W. Beyn, An integral method for solving nonlinear eigenvalue problems. *Linear Alg. Appl.*, (2012), 3839-3863.

[3] F. Cakoni, D. Colton, P. Monk and J. Sun, The inverse electromagnetic scattering problem for anisotropic media, *Inverse Probl.*, **26** (2010), 074004.

[4] F. Cakoni and H. Haddar, Transmission eigenvalues in inverse scattering theory, *G. Uhlmann editor, Inside Out II, 60, MSRI Publications*, 2012, 526-578.

[5] F. Cakoni, P. Monk and J. Sun, Error analysis of the finite element approximation of transmission eigenvalues, *Comput. Methods Appl. Math.*, **14** (2014), 419-427.

[6] P. Ciarlet and J. Lions, *Handbook of Numerical Analysis, vol. II*, North-Holland, 2000.

[7] D. Colton and R. Kress, *Inverse Acoustic and Electromagnetic Scattering Theory, 2nd ed.*, Springer-Verlag, New York, 1998.

[8] D. Colton, P. Monk and J. Sun, Analytical and computational methods for transmission eigenvalues, *Inverse Probl.*, **26** (2010), 045011.

[9] D. Colton, L. Päivärinta and J. Sylvester, The interior transmission problem, *Inverse Probl. Imaging*, **1** (2007), 13-28.

[10] G. Hsiao, F. Liu, J. Sun and L. Xu, A coupled BEM and FEM for the interior transmission problem in acoustics, *J. Comput. Appl. Math.*, **235** (2011), 5213-5221.

[11] R. Huang, A. Struthers, J. Sun and R. Zhang, Recursive integral method for transmission eigenvalues, *J. Comput. Phys.*, **327** (2016), 830-840.

[12] X. Ji and J. Sun, A multi-level method for transmission eigenvalues of anisotropic media, *J. Comput. Phys.*, **255** (2013), 422-435.

[13] X. Ji, J. Sun and T. Turner, A mixed finite element method for Helmholtz transmission eigenvalues, *ACM T. Math. Software*, **38** (2012), Algorithm 922.

[14] X. Ji, J. Sun and H. Xie, A multigrid method for Helmholtz transmission eigenvalue problems, *J. Sci. Comput.*, **60** (2014), 276-294.

[15] X. Ji, Y. Xi and H. Xie, Nonconforming finite element method for the transmission eigenvalue problem, *Adv. Appl. Math. Mech.*, **9** (2017), 92-103.

[16] T. Kato, *Perturbation Theory of Linear Operators*, Springer-Verlag, 1966.

[17] A. Kleefeld, A numerical method to compute interior transmission eigenvalues, *Inverse Probl.*, **29** (2013), 104012.

[18] A. Lechleiter and M. Rennoch, Inside-outside duality and the determination of electromagnetic interior transmission eigenvalues, *SIAM J. Math. Anal.*, **47** (2015), 684-705.

[19] T. Li, W. Huang, W. Lin and J. Liu, On spectral analysis and a novel algorithm for transmission eigenvalue problems, *J. Sci. Comput.*, **64** (2015), 83-108.

[20] L. Morley, The triangular equilibrium problem in the solution of plate bending problems, *Aero. Quart.*, **19** (1968), 149-169.

[21] E. Polizzi, Density-matrix-based algorithms for solving eigenvalue problems, *Phys. Rev. B*, **79** (2009), 115112 .

[22] T. Sakurai and H. Sugiura, A projection method for generalized eigenvalue problems using numerical integration, *Proceedings of the 6th Japan-China Joint Seminar on Numerical Mathematics, J. Comput. Appl. Math.*, **159** (2003), 119-128.

[23] J. Sun, Iterative methods for transmission eigenvalues, *SIAM J. Numer. Anal.*, **49** (2011), 1860-1874.

[24] J. Sun, An eigenvalue method using multiple frequency data for inverse scattering problems, *Inverse Probl.*, **28** (2012), 025012.

[25] J. Sun and A. Zhou, *Finite Element Methods for Eigenvalue Problems*, CRC Press, 2016.

[26] X. Wu and W. Chen, Error estimates of the finite element method for interior transmission problems, *J. Sci. Comput.*, **57** (2013), 331-348.